



Cite this: *Chem. Commun.*, 2024, 60, 11837

Received 28th August 2024,
Accepted 16th September 2024

DOI: 10.1039/d4cc04414b

rsc.li/chemcomm

Development of chemiluminescent systems and devices for analytical applications

Zhiyong Dong, ^{ab} Fangxin Du, ^c Saima Hanif, ^d Yu Tian*^{ab} and Guobao Xu *^{ab}

Chemiluminescence (CL) refers to the light-emitting phenomenon resulting from chemical reactions. Due to its simplicity in terms of instrumentation and high sensitivity, CL plays a critical role in analytical chemistry and has developed rapidly in recent years. In this review, we discuss the efforts made by our group in the field of CL. This includes exploring new luminophores that function under neutral pH conditions, developing oxidant- and reactive oxygen species-based coreactants (e.g. artemisinin and thiourea dioxide) for luminol and lucigenin CL, utilizing nanomaterial-based CL signal amplification and employing innovative ultrasound devices for CL and their analytical applications. We discussed the CL amplification mechanisms of these systems in detail. Finally, we summarize the challenges and prospects for the future development of CL.

1. Introduction

Chemiluminescence (CL) refers to the phenomenon of light emission resulting from the return of the excited state intermediates, generated from the chemical reactions, to their ground state.¹ The origin of CL can be traced back to 1877 when Radziszewski *et al.* discovered that lophine could react with hydrogen peroxide (H_2O_2) under alkaline conditions to emit green

light.² Since then, typical CL luminophores such as luminol,³ lucigenin⁴ and tris(bipyridine)ruthenium ($Ru(bpy)_3^{2+}$)⁵ have been reported. However, the early development of CL techniques was slow due to the low intensity of most CL systems and the lack of sensitive luminescence measurement instruments. The CL method flourished after the introduction of the photomultiplier tube (PMT). Recently, CL has become a powerful analytical tool and has been widely applied in fields such as food and drug analyses,^{6–8} environmental monitoring,^{9–11} nucleic acid analysis,¹² immunoassay,¹³ and CL bioimaging.¹⁴ This is because the CL technique does not require an external excitation light source and features a simple device with high sensitivity, a wide linear range, and fast detection speed compared to other optical methods.

However, conventional CL systems face practical limitations due to their poor stability and the low quantum efficiency of CL

^a State Key Laboratory of Electroanalytical Chemistry, Changchun Institute of Applied Chemistry, Chinese Academy of Sciences, Changchun, Jilin 130022, PR China

^b University of Science and Technology of China, Hefei 230026, China.
E-mail: tianyu@ciac.ac.cn, guobaoxu@ciac.ac.cn

^c School of Chemistry and Material Science, Huaipei Normal University, Huaipei 235000, China

^d Department of Biological Sciences, National University of Medical Sciences, The Mall Road, Rawalpindi, Punjab 46000, Pakistan



Zhiyong Dong

Zhiyong Dong obtained his BSc degree from Huazhong Agricultural University in 2020. Currently he is a PhD student of Prof. Guobao Xu at the State Key Laboratory of Electroanalytical Chemistry, Changchun Institute of Applied Chemistry, Chinese Academy of Sciences, China. His research interests focus on chemiluminescence and electrochemiluminescence sensing.



Fangxin Du

Fangxin Du obtained her BSc in applied chemistry from the Hefei University of Technology. She received her PhD degree under the guidance of Prof. Guobao Xu at the University of Science and Technology of China. She is currently working at Huaipei Normal University as a lecturer. Her research interests focus on chemiluminescence, electrochemiluminescence, and immuno-sensing.



luminophores. To address these issues, extensive research has been conducted, including searching for substitute luminophores and coreactants,^{15,16} synthesis of novel luminophores and their derivatives,^{17,18} finding highly efficient catalytic nanomaterials,^{19,20} and exploration of new catalytic CL modes.²¹ In this feature article, we systematically describe our efforts to construct new CL systems and their analytical applications. This includes the exploration of new luminophores, coreactants and their novel analytical applications, nanomaterial-based signal amplification strategies, and CL enhancement driven by mini ultrasound devices. Additionally, we provide detailed background information and highlight significant contributions from other groups. This manuscript aims to advance the development of CL methods in analytical chemistry.



Saima Hanif

Applied Chemistry, Chinese Academy of Sciences from 2013 to 2014 supported by the CAS-TWAS postgraduate fellowship. Currently, she is working as an assistant Professor in the National University of Medical Sciences.



Yu Tian

analytical Chemistry. His research includes the precise synthesis and optical applications of nanomaterials.

2. Exploration of coreactants and luminophores

Luminophores and coreactants are crucial components of CL systems. CL arises from energetic intermediates generated by chemical reactions between luminophores and coreactants. Consequently, the intensity of CL is directly influenced by the properties of these components. In this section, we primarily discuss our recent exploration of novel luminophores and coreactants along with their analytical applications.

2.1 Luminol based new CL systems

Luminol is one of the most popular CL luminophores owing to its simple structure, ease of synthesis, good water solubility, high stability, and luminescence efficiency. Luminol can generate CL at a wavelength of 425 nm²² by reacting with typical oxidants like potassium permanganate (KMnO₄),²³ sodium hypochlorite (NaClO),²⁴ H₂O₂, and others. However, coreactants such as KMnO₄ and NaClO with strong oxidizing properties may be affected by various factors in practical detection, which in turn influence the CL accuracy of analyte detection. Although H₂O₂ has moderate oxidizing ability, it is intrinsically unstable. Additionally, luminol CL generally requires alkaline conditions, which accelerates the decomposition of H₂O₂, leading to poor CL signal stability. Therefore, it is necessary to develop alternative luminol coreactants.

2.1.1 Peroxide based coreactants. Generally, peroxides like H₂O₂ can react with luminol to emit CL. Therefore, chemicals that have peroxide bonds or stimulate the generation of peroxide bond-based intermediates can be chosen as coreactants to develop CL sensors.

Artemisinin and its derivatives are natural endoperoxides.²⁵ The luminol/artemisinin CL system without catalysts was reported by our group in 2021.²⁶ As shown in Fig. 1A, the CL intensity of the luminol/artemisinin system remains unchanged over time because the internal peroxide bond



Guobao Xu

Guobao Xu received his BSc from Jilin University, MSc from Xiamen University, and PhD from the Changchun Institute of Applied Chemistry, Chinese Academy of Sciences. After postdoctoral research at the University of Hong Kong, Hong Kong Polytechnic University, and JST-NTT, he joined the Changchun Institute of Applied Chemistry in 2004. He has co-authored more than 350 papers. His research interests include electrochemiluminescence, chemiluminescence, electroanalysis, electrocatalysis, electrochemical devices, biosensors, precise nanomaterial synthesis, and metal ion batteries.



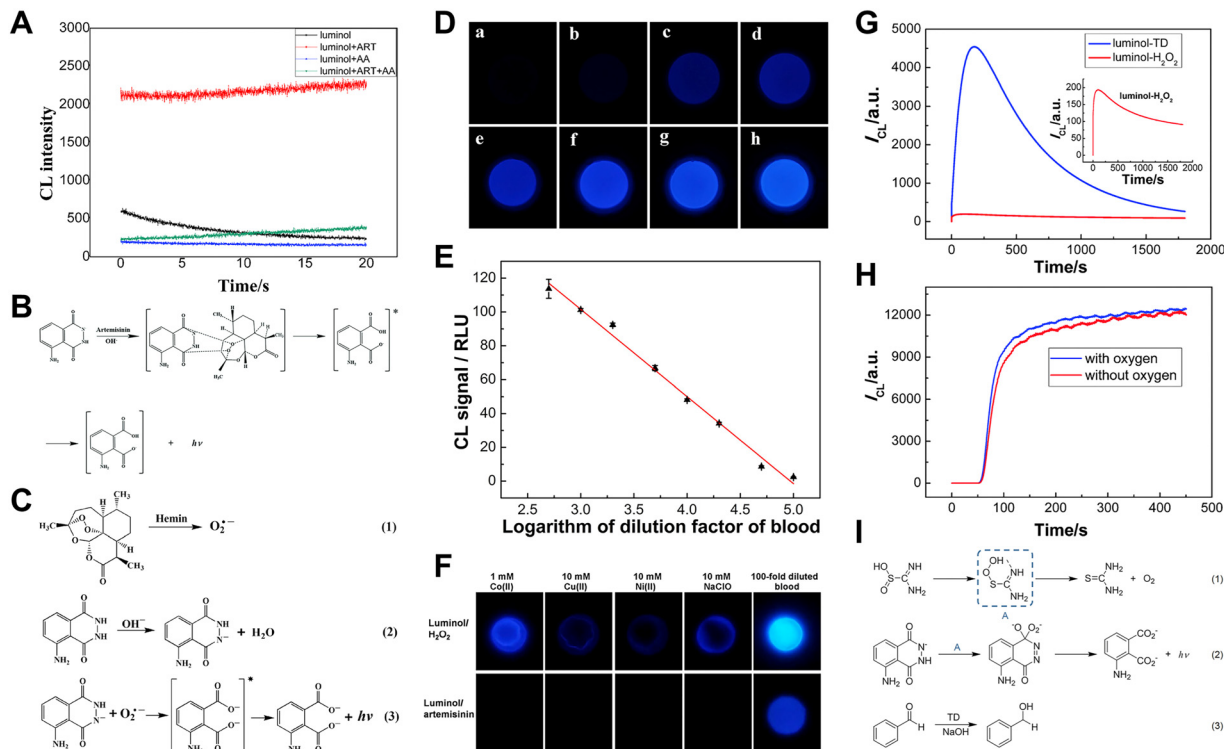


Fig. 1 (A) The CL intensity–time curves of the luminol, luminol/artemisinin, luminol/ascorbic acid (AA) and luminol/artemisinin/AA systems. [Luminol]: 1 mM; [artemisinin]: 4 mM; [AA]: 1 μ M; pH: 12.30; PMT voltage: –1100 V. (B) The CL reaction mechanism between luminol and artemisinin. Reprinted with permission from ref. 26, Copyright 2021 Royal Society of Chemistry. (C) The CL mechanism of the luminol/artemisinin/hemin system. (D) CL images of blood samples of different dilution factors: (a) 100 000, (b) 50 000, (c) 20 000, (d) 10 000, (e) 5000, (f) 2000, (g) 1000, and (h) 500. (E) The relationship curve of CL intensities versus the logarithm of the dilution factors of blood. (F) Comparison between luminol/H₂O₂ and luminol/artemisinin CL systems in distinguishing blood from NaClO and common metal ions Co²⁺, Cu²⁺, and Ni²⁺. [luminol]: 1.0 mM; [H₂O₂]: 1.0 mM; [artemisinin]: 5.0 mM. Reprinted with permission from ref. 27, Copyright 2017 American Chemical Society. (G) The CL intensity–time curves of the luminol/H₂O₂ and luminol/TD systems, [luminol]: 0.1 mM; [TD]: 1 mM; [H₂O₂]: 1 mM; PMT voltage: –700 V. (H) The effect of dissolved oxygen on the luminol/TD system, [luminol]: 0.1 mM; [TD]: 10 mM; PMT voltage: –700 V. Reprinted with permission from ref. 28, Copyright 2015 Royal Society of Chemistry. (I) The proposed CL mechanism for the luminol/TD system. Reprinted with permission from ref. 29, Copyright 2022 Royal Society of Chemistry.

within artemisinin is stable and decomposes slowly under alkaline conditions. The CL mechanism of luminol/artemisinin is shown in Fig. 1B. Luminol is oxidized by artemisinin and produces excited state intermediates (3-aminophthalate anions), which then return to their ground state accompanied by CL emission.

In addition, previous reports have described the ability of artemisinin to enhance the luminol CL in the presence of catalysts like hemin.^{30,31} Based on this finding, on-site smartphone-based visual detection of hemin and bloodstains was proposed.²⁷ Under the catalysis of hemin, the peroxide bond of artemisinin breaks and generates superoxide anions ($O_2^{\bullet-}$), which then react with deprotonated luminol and emit blue light (Fig. 1C).

Utilizing the luminol/artemisinin/hemin system, CL signals of blood samples can be captured in the darkroom using a smartphone (Fig. 1D). Moreover, the relationship between CL intensity and the blood dilution factor was investigated. The results (Fig. 1E) showed that up to 100 000 times diluted blood could be detected using the smartphone-based luminol/artemisinin/hemin system. As compared to the typical

luminol/H₂O₂ system for bloodstain detection, luminol/artemisinin is less susceptible to other oxidizing agents and common ions (Fig. 1F). Therefore, artemisinin and its analogue as coreactants for luminol are highly promising for bloodstain CL detection.

Building on the luminol/artemisinin/hemin CL system, artesunate was employed as the luminol coreactant to improve the poor water solubility of artemisinin.³² In contrast, their CL mechanisms are similar, employing catalysts to accelerate the breaking of the peroxide bond to form reactive oxygen species (ROS). However, artesunate is more readily available for real tests due to its better water solubility and CL intensity.

As mentioned above, chemicals capable of generating peroxide bond-based intermediates can also act as coreactants for luminol CL.

Thiourea dioxide (TD), an environmentally friendly reductant, was reported by our group as a coreactant for luminol CL for the first time.²⁸ Compared to the typical luminol/H₂O₂ system, the CL intensity was enhanced by 23 times (Fig. 1G). To explore the CL mechanism of the luminol/TD system, we investigated the effect of oxygen on luminol CL. As shown in Fig. 1H, no obvious change in CL intensity was observed after

removing dissolved oxygen, indicating that CL enhancement is irrelevant to oxygen. Combining our experiments with previous research on TD,³³ the corresponding mechanism can be deduced as shown in Fig. 1I. In an alkaline solution, TD decomposes to produce hydroperoxide intermediates, which then react with luminol to enhance CL intensity. Based on the reduction of carbonyl compounds by TD, a signal-off CL sensor for a typical carbonyl compound (benzaldehyde) was established.²⁹

Besides TD, *N*-hydroxy succinimide (NHS) can also produce peroxides and subsequently react with luminol under alkaline conditions.³⁴ Thus, NHS can also serve as a coreactant for luminol.³⁵ The CL intensity of the luminol/NHS system was enhanced 22 folds compared to the classical luminol/H₂O₂ system.

2.1.2 Coreactant induced ROS generation for luminol CL.

The enhancement of luminol CL can be achieved by promoting the production of ROS. Therefore, chemicals that convert oxygen to ROS can be used as coreactants for luminol CL.

Fluorescamine is a classical fluorescent probe and can react with primary amines to yield highly fluorescent products. Therefore, it has been widely used in the assay of amino acids, peptides and proteins.³⁶ We found that fluorescamine can react with luminol and produce CL.³⁷ As shown in Fig. 2A, when polyvinylpyrrolidone (PVP) was added, luminol CL was further increased. The CL spectrum shown in Fig. 2B indicates that the maximum CL wavelength was at 440 nm, which is consistent with typical luminol CL emission. To further investigate the mechanism of the luminol/fluorescamine/PVP system, the oxygen in the solution was removed, and common radical scavengers were adopted. As shown in Fig. 2C and D, the removal of oxygen and the addition of superoxide dismutase (SOD) almost completely quench the CL intensity, suggesting that oxygen is necessary for the luminol/fluorescamine/PVP system and fluorescamine may facilitate the conversion of oxygen to O₂^{•-}. As for the CL enhancement by PVP, it is possibly attributed to its ability to stabilize the free radicals. The CL mechanism of luminol/fluorescamine/PVP is shown in Fig. 2E.

2.1.3 In situ generation of oxidants for luminol CL.

As noted above, oxidants can react with luminol and emit CL. *In situ* formation of oxidants is an efficient way to induce luminol CL.

Silicotungstic acid (STA) is a kind of heteropoly acid commonly used as a catalyst in organic chemistry.^{38,39} It remains stable under acidic and mildly alkaline conditions but decomposes into silicate ions and tungsten trioxide (WO₃) under strong alkaline conditions.^{40,41} As depicted in Fig. 3A and B, the *in situ* generated WO₃ can act as a coreactant to induce luminol CL due to its oxidizability. The luminol/STA CL system exhibits a significantly better CL effect (65 times) compared to the luminol/H₂O₂ system.⁴²

2.2 Lucigenin based new CL systems

Lucigenin (*N,N'*-dimethyl-9,9'-biacridinium dinitrate) is the most representative CL reagent among acridine esters and

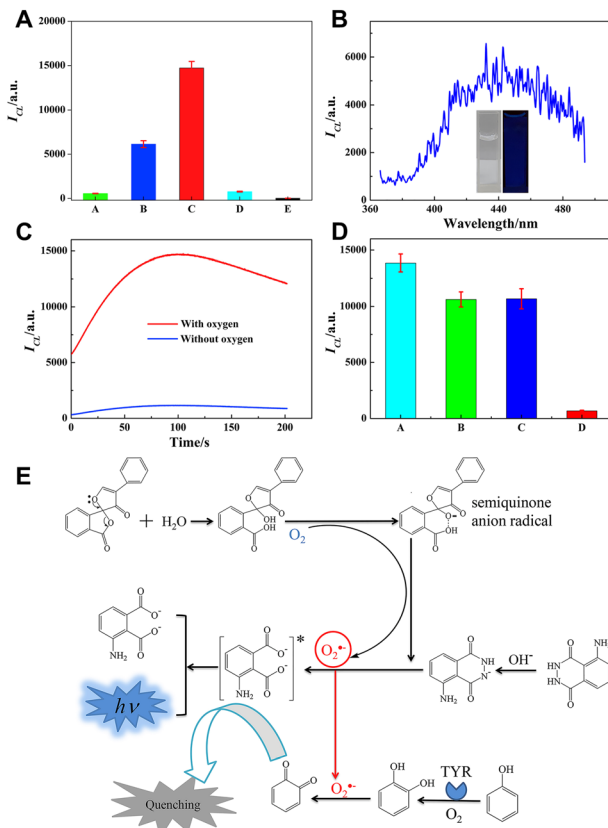


Fig. 2 (A) CL intensity of different systems. (A) luminol; (B) luminol/fluorescamine; (C) luminol/fluorescamine/PVP; (D) luminol/PVP and (E) fluorescamine/PVP. (B) CL spectrum of the luminol/fluorescamine/PVP system. The inset shows the comparison of CL images before and after adding luminol. (C) The CL kinetic curves of the luminol/fluorescamine/PVP system in the presence and absence of oxygen. (D) CL intensity of luminol/fluorescamine/PVP in the absence (A) and presence of radical scavengers (B) 1.0 mM thiourea, (C) 1.0 mM NaN₃, and (D) 0.1 μ g mL⁻¹ SOD. (E) Mechanism of the luminol/fluorescamine/PVP CL system. PBS, 0.1 M, pH 9.0; [luminol]: 0.1 mM; [fluorescamine]: 0.1 mM; [PVP]: 0.3 mg mL⁻¹. Reprinted with permission from ref. 37, Copyright 2020 Elsevier.

one of the most widely used CL luminophores in the field of analytical chemistry. H₂O₂ is the most classical CL coreactant for lucigenin. Under alkaline conditions, lucigenin reacts with H₂O₂, emitting light with a wavelength of approximately 490 nm. Generally, the mechanisms of lucigenin-based CL systems are similar to Scheme 1. Initially, lucigenin converts to lucigenin cation radicals in an alkaline solution. These radicals are then oxidized to form lucigenin dioxetane. Subsequently, lucigenin dioxetane decomposes into excited state intermediates, which return to the ground state with light emission.

2.2.1 Oxidant based new lucigenin CL systems. According to the CL mechanism of lucigenin, the principles for identifying coreactants are similar to those for luminol. This means that chemicals capable of forming oxidants or intermediates with oxidizing properties or converting oxygen to ROS have the potential to act as coreactants for lucigenin. Consequently, some coreactants for luminol CL can also function for



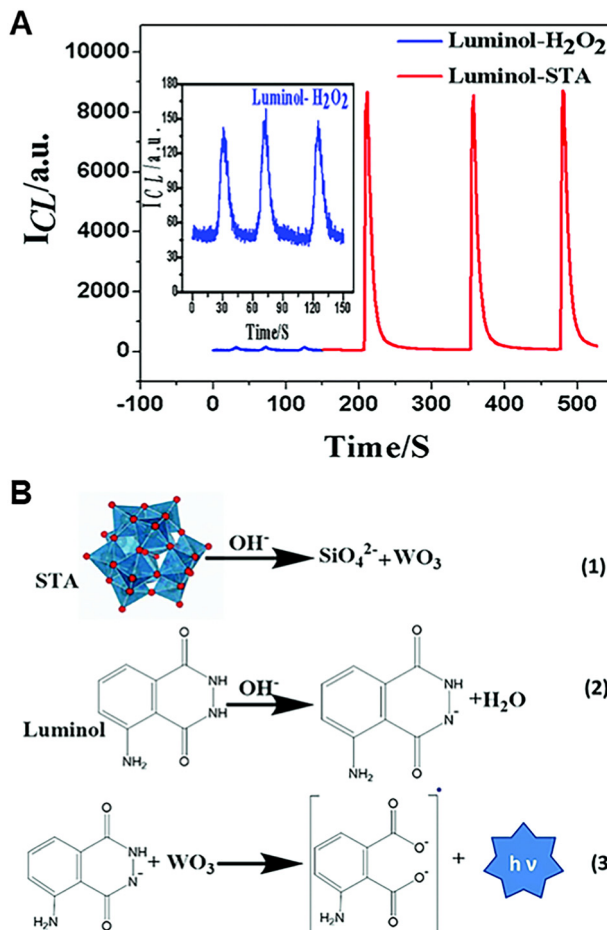
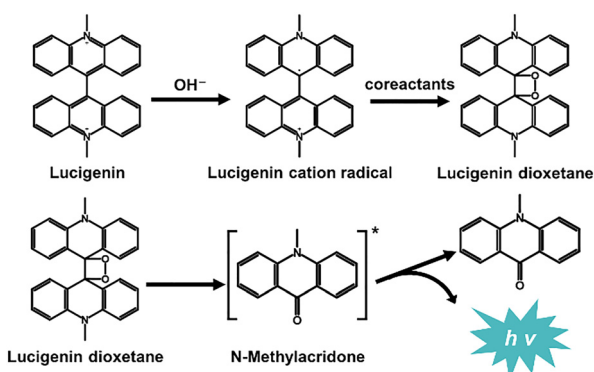


Fig. 3 (A) The relationship between CL intensities and time for the luminol/H₂O₂ system and luminol/STA system [luminol]: 10 μ M; [STA]: 2 mM; [H₂O₂]: 2 mM; pH: 12.0; PMT voltage: -950 V. (B) The CL mechanism of the luminol/STA system. Reprinted with permission from ref. 42, Copyright 2020 Royal Society of Chemistry.



Scheme 1 Mechanism of lucigenin-based CL systems.

lucigenin CL. For instance, after the report of TD as the coreactant for luminol, its reaction with lucigenin has also been investigated.⁴³ As depicted in Fig. 4A, the CL intensity is about 75 times higher compared to that of the lucigenin/H₂O₂ CL system. The mechanism of the lucigenin/TD system (Fig. 4B) is

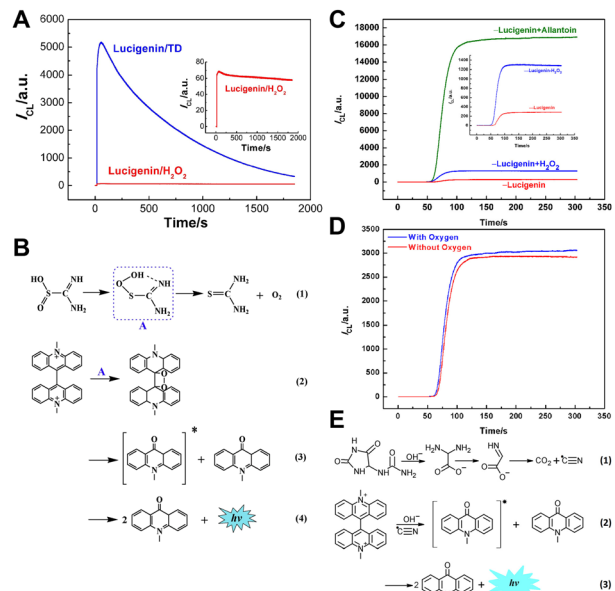


Fig. 4 (A) The CL intensity-time curves of the lucigenin/H₂O₂ and lucigenin/TD systems. Inset: enlarged CL intensity-time curve of the lucigenin/H₂O₂ system. [Lucigenin]: 10.0 μ M; [TD]: 1.0 mM; [H₂O₂]: 1.0 mM; [NaOH]: 0.5 M; PMT voltage: -700 V. (B) Reaction mechanism of the lucigenin/TD CL system. Reprinted with permission from ref. 43, Copyright 2016 Elsevier. (C) CL intensity-time curves of the lucigenin, lucigenin/H₂O₂ and lucigenin/allantoin systems. The inset focuses on the enlarged CL intensity/time curve of lucigenin and lucigenin/H₂O₂ systems. 1.5 M NaOH, 0.1 mM lucigenin, 2 mM H₂O₂, and 2 mM allantoin. PMT voltage: -800 V. (D) CL kinetic profiles in the presence and absence of oxygen. 1.5 M NaOH, 0.1 mM lucigenin and 2 mM allantoin. PMT voltage: -600 V. (E) Possible mechanism of the lucigenin/allantoin CL system. Reprinted with permission from ref. 44, Copyright 2017 American Chemical Society.

attributed to the formation of peroxide intermediates with oxidizing properties.

Besides TD, allantoin (5-ureidohydantoin) was selected as a coreactant due to its ability to generate oxidant radicals in the alkaline medium.⁴⁴ Under optimal conditions, the CL intensity of the lucigenin/allantoin system was about 17 times higher than that of the classic lucigenin/H₂O₂ system (Fig. 4C). Additionally, the CL intensities were compared before and after deoxygenation. As shown in Fig. 4D, there is little difference in the CL intensity, proving that the CL signal of lucigenin/allantoin is independent of oxygen. Therefore, the CL mechanism of lucigenin/allantoin is proposed in Fig. 4E. The allantoin decomposed, forming cyano radicals, which then reacted with lucigenin to emit light. Based on the lucigenin/allantoin system, a rapid and simple CL method for allantoin detection was developed with a detection limit of 0.03 μ M, and allantoin in human eye drops and real urine samples was successfully determined.

2.2.2 Promoting ROS production for new lucigenin CL systems. Chemicals that convert ROS from oxygen to realize lucigenin CL enhancement can also be recognized as coreactants for lucigenin. Dithiothreitol (DTT), also known as Cleland's reagent, was used for lucigenin CL in 2022.⁴⁵ As illustrated in Fig. 5, DTT is a better coreactant for lucigenin than H₂O₂.

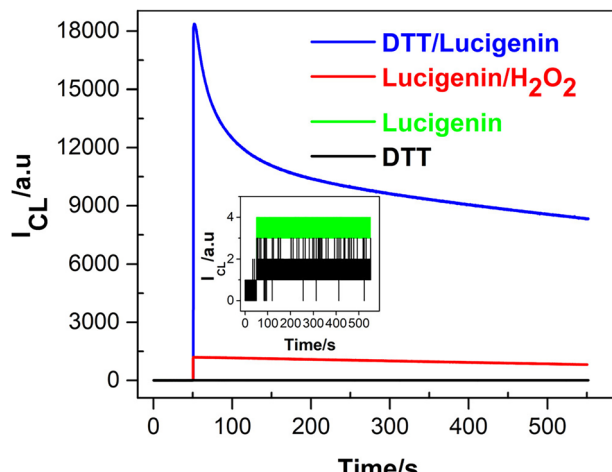


Fig. 5 CL intensity versus time profiles for the systems of lucigenin/DTT, lucigenin/H₂O₂, lucigenin, and DTT. Inset: enlarged CL emissions of DTT and lucigenin. [Lucigenin]: 0.1 mM; [DTT]: 1.0 mM; [H₂O₂]: 1.0 mM; 0.1 M PBS (pH 11); PMT voltage: -750 V. Reprinted with permission from ref. 45, Copyright 2022 American Chemical Society.

In addition, the effect of oxygen was investigated in Fig. 6A; the CL intensity decreases completely without oxygen, indicating that oxygen is involved in the CL process of the lucigenin/DTT system. To further investigate the CL mechanism, common radical scavengers were used to explore the ROS. As Fig. 6B describes, CL intensity is quenched with the addition of SOD, indicating that the O₂^{•-} radicals are the main ROS involved in the lucigenin CL process. According to these experimental results and the typical lucigenin CL process, the CL mechanism of lucigenin/DTT is proposed in Fig. 6C. In the presence of DTT, oxygen was activated and transformed to O₂^{•-}, which then reacts with lucigenin and emits luminescence.

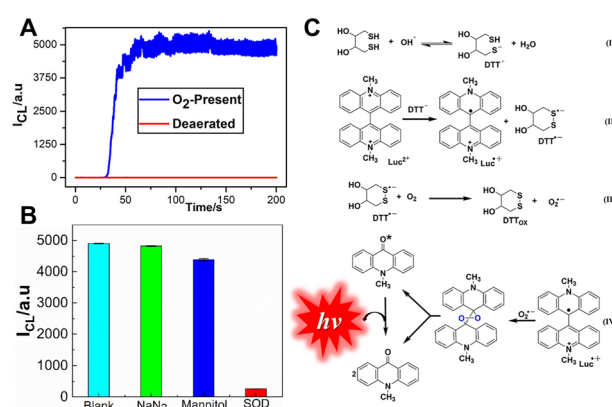


Fig. 6 (A) The effect of dissolved oxygen on the DTT/lucigenin system. Flow rate: 1.5 mL min⁻¹; [Lucigenin]: 10 μ M; [DTT]: 0.3 mM; PMT voltage: -750 V. (B) Influences of radical scavengers on the DTT/lucigenin CL system. [Lucigenin]: 0.1 mM; [DTT]: 0.3 mM; [NaN₃]: 0.3 mM; [mannitol]: 0.3 mM; [SOD]: 0.5 μ g mL⁻¹. 0.1 M PBS, pH 11. (C) CL mechanism of the DTT/lucigenin system. Reprinted with permission from ref. 45, Copyright 2022 American Chemical Society.

2.3 New luminophores for CL

Luminophores are also important components in the CL system. Typical luminophores like luminol and lucigenin commonly require strong alkaline conditions. However, most analytical assays like immunosensing and enzyme-based analysis require mild neutral conditions. Although Ru(bpy)₃²⁺ works under neutral conditions, it requires electrical energy to emit light efficiently. Therefore, the exploration of CL luminophores working under mild conditions is important.

The 9-mesityl-10-methylacridinium ion (Acr⁺-Mes) is a donor-acceptor molecule consisting of a mutually perpendicular acridine ion (Acr⁺) and mesitylene (Mes). Due to its special structure and the redox properties of the excited state, it does not depend on the strong alkaline conditions to generate an electron transfer state, making it promising for CL analysis under weakly alkaline or neutral conditions. Under mild conditions, its CL phenomenon with potassium peroxy-monosulfate (KHSO₅) has been reported by our group recently (Fig. 7).

For the Acr⁺-Mes/KHSO₅ system, several kinds of radicals, including sulfate radicals (SO₄^{•-}) and ROS, were produced (Fig. 8A-C). However, there are small changes in the CL intensity when adding H₂O₂ to the Acr⁺-Mes solution (Fig. 8D), which indicates that the SO₄^{•-} radicals are the main radicals to react with Acr⁺-Mes. Based on the generation of SO₄^{•-} and ROS from the accelerated decomposition of KHSO₅ catalyzed by Co²⁺ (Fig. 8E), a CL sensor for Co²⁺ detection was proposed using the Acr⁺-Mes/KHSO₅ system.

3. Nanomaterial based CL signal amplification

Nanomaterials have been widely used in analytical chemistry due to their good biocompatibility, easy dispersion, excellent catalytic properties, *etc.* In the past few decades, different kinds of nanomaterials were synthesized for CL signal amplification and sensing.^{46,47} For example, Peng *et al.* achieved efficient

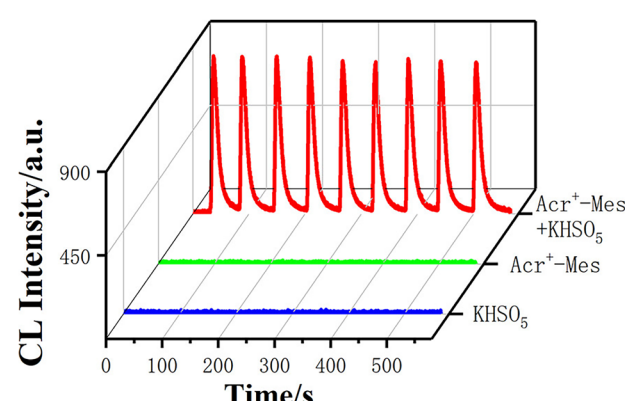


Fig. 7 CL intensity-time curves of KHSO₅, Acr⁺-Mes, and Acr⁺-Mes/KHSO₅ systems. [Acr⁺-Mes]: 0.1 mM; [KHSO₅]: 2 mM; [PBS]: 0.1 M, pH = 7; PMT voltage: -900 V. Reprinted with permission from ref. 15, Copyright 2023 American Chemical Society.



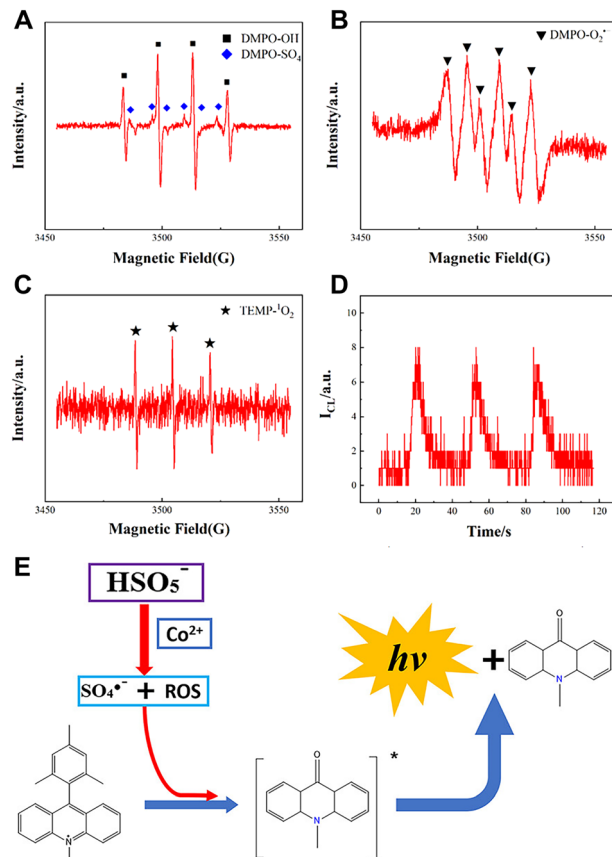
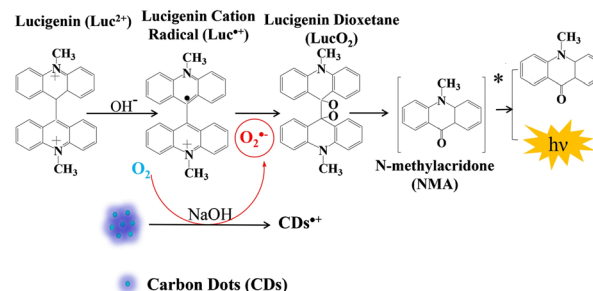


Fig. 8 ESR spectra of (A) $\text{OH}^\bullet/\text{SO}_4^{\bullet-}$, (B) $\text{O}_2^{\bullet-}$ and (C) $^1\text{O}_2$ in the Acr^+ –Mes/KHSO₅ system. (D) CL intensity of the Acr^+ –Mes/H₂O₂ system. (E) CL mechanism of the Acr^+ –Mes/H₂O₂ system and the detection of Co^{2+} . [Acr^+ –Mes]: 0.1 mM; [KHSO_5]: 2 mM; [H_2O_2]: 2 mM; [PBS]: 0.1 M, pH = 7.0. PMT voltage: –900 V. Reprinted with permission from ref. 15, Copyright 2023 American Chemical Society.

luminescence of the luminol/H₂O₂ system and realized dopamine detection using Fe/Co bimetallic MOF nanosheets (NSs) synthesized at room temperature.⁴⁸ Huang *et al.* synthesized molybdenum disulfide NSs and realized luminol CL without the addition of oxidants.⁴⁹ In this section, the nanomaterial-based CL signal amplification strategies proposed by our group are reviewed.

As a classical non-metallic nanomaterial, carbon dots (CDs) are widely used in extensive fields, especially in the fluorescence field, due to their low toxicity, good water solubility, nice biocompatibility, and tunable fluorescence.⁵⁰ Previous reports have proved that $\text{O}_2^{\bullet-}$ can be generated by the electron transfer process between CDs and dissolved oxygen in sodium hydroxide (NaOH) solutions.⁵¹ Utilizing this principle, lucigenin CL enhancement was achieved in the presence of CDs.⁵² The CL mechanism of lucigenin/CDs is shown in Scheme 2. $\text{O}_2^{\bullet-}$ radicals are produced from dissolved oxygen under the catalysis of CDs in NaOH solution, which then reacts with lucigenin cation radicals and realizes lucigenin CL signal amplification.

Nanozymes have attracted much attention due to the combination of the excellent properties of nanomaterials with the



Scheme 2 Schematic representation of the lucigenin–CD CL system in NaOH solution. Reprinted with permission from ref. 52, Copyright 2019 Springer Nature.

high catalytic activity of enzymes.^{53,54} Compared with natural enzymes, nanozymes are of low-cost and stable, and thus have a wide range of applications in biosensing. As a class of nanozymes, transition-metal-based nanozymes show great potential for CL because of their stability, excellent catalytic properties,

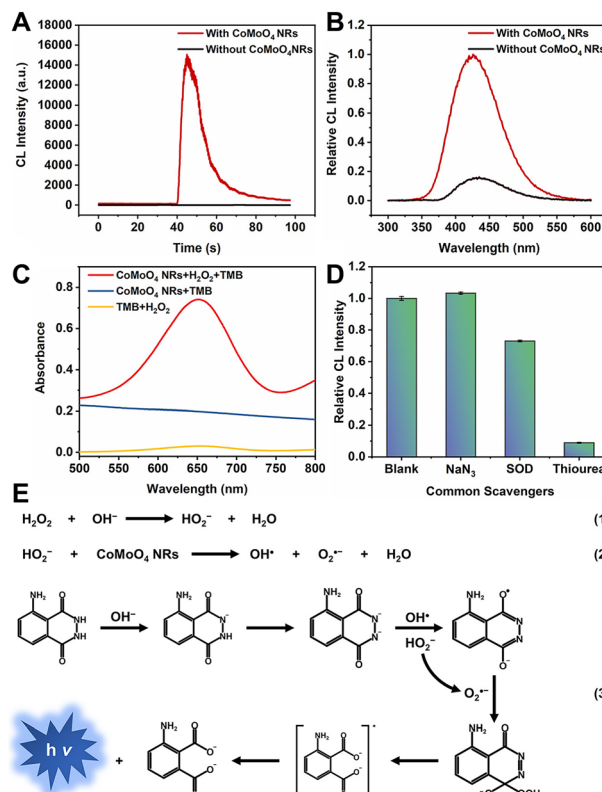


Fig. 9 (A) CL intensity–time curves and (B) CL spectra of the luminol/H₂O₂ system in the absence and presence of CoMoO₄ NRs. CBS pH 11.0, [luminol]: 1 μM ; [H₂O₂]: 50 μM ; [CoMoO₄ NRs]: 20 $\mu\text{g mL}^{-1}$. (C) UV-vis absorption spectra of TMB/H₂O₂, CoMoO₄ NRs/H₂O₂, and CoMoO₄ NRs/H₂O₂/TMB systems. NaAc/HAc buffer solution pH 4.0, [TMB]: 0.1 mM; [H₂O₂]: 25 mM; [CoMoO₄ NRs]: 50 $\mu\text{g mL}^{-1}$. (D) Relative CL intensity of luminol/H₂O₂/CoMoO₄ NRs with common radical scavengers including 1 mM NaAc, 5 $\mu\text{g mL}^{-1}$ SOD, and 1.0 mM thiourea. CBS pH 11.0; [luminol]: 1 μM ; [H₂O₂]: 50 μM ; [CoMoO₄ NRs]: 20 $\mu\text{g mL}^{-1}$. (E) CL mechanism of the luminol/H₂O₂/CoMoO₄ NR system. Reprinted with permission from ref. 61, Copyright 2024 American Chemical Society.

good biocompatibility, and facile synthesis.^{55,56} Under suitable conditions, nanozymes are able to induce the production of ROS from oxygen or H_2O_2 .^{57,58} It has been reported that CoMoO_4 possesses excellent peroxidase-mimicking activity.^{59,60} Utilizing this property, CoMoO_4 nanorods (NRs) were adopted to enhance the CL of the luminol/ H_2O_2 system.⁶¹ The CL intensity of luminol/ H_2O_2 under optimal conditions was enhanced 750-fold under the catalysis of CoMoO_4 NRs (Fig. 9A). The wavelength of luminol/ $\text{H}_2\text{O}_2/\text{CoMoO}_4$ NRs is 426 nm (Fig. 9B), consistent with typical luminol CL. In addition, the peroxidase-mimicking activity of CoMoO_4 NRs was confirmed by the TMB color development experiment (Fig. 9C). Further experiments were carried out to detect the free radicals in the CL process (Fig. 9D) of the luminol/ $\text{H}_2\text{O}_2/\text{CoMoO}_4$ NR system, and the CL mechanism is presented in Fig. 9E.

Multimetallic nanozymes usually exhibit superior catalytic effects as compared to their monometallic counterparts due to the synergistic effect of central metals. In 2023, our group developed trimetallic metal-organic xerogels (MOXs) *via* a mild one-step procedure at room temperature and subsequent freeze-drying using Fe(III), Co(II), Ni(II) as central metals and 1,3,5-benzenetricarboxylic acid (H_3BTC) as the ligand (Fig. 10A).⁶² The trimetallic MOXs exhibit good peroxidase mimetic activity (Fig. 10B) and can enhance the CL signals of the luminol/ H_2O_2 system by more than 3000 times (Fig. 10C). Dopamine can quench the CL of the luminol/ $\text{H}_2\text{O}_2/\text{FeCoNi-MOX}$ system. Therefore, a highly sensitive CL sensor for dop-

amine detection was proposed using the luminol/ $\text{H}_2\text{O}_2/\text{FeCoNi-MOX}$ CL system.

Furthermore, to avoid the influence of CL intensity resulting from H_2O_2 , the nanomaterial with oxidase-mimicking activity was used to promote the generation of ROS from oxygen and enhance CL. FeOOH NRs were adopted to enhance the luminol CL without adding any oxidants (Fig. 11).⁶³

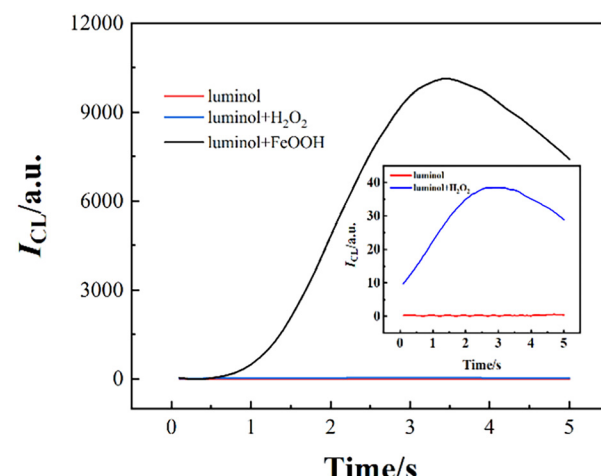


Fig. 11 The CL intensity–time curves of luminol, luminol/ H_2O_2 and luminol/FeOOH systems. [Luminol]: 100 μM ; [FeOOH]: 25 $\mu\text{g mL}^{-1}$; [H_2O_2]: 1 μM ; [pH]: 10.0. Reprinted with permission from ref. 63, Copyright 2023, American Chemical Society.

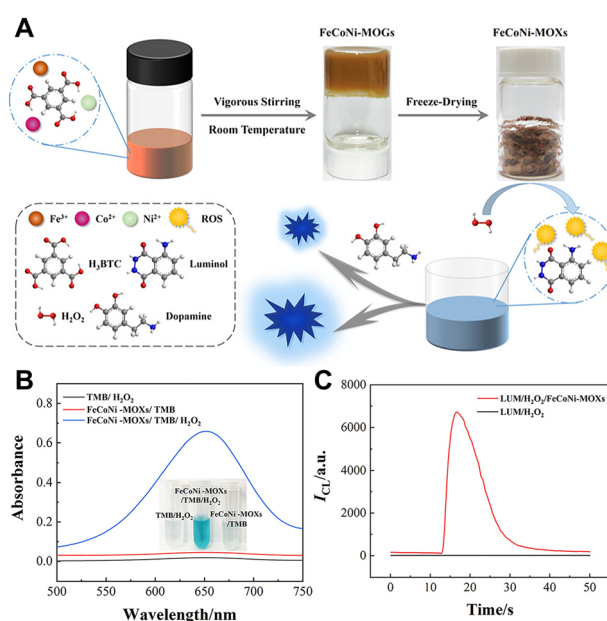


Fig. 10 (A) Schematic of the synthesis of FeCoNi-MOXs and its mechanism to enhance luminol/ H_2O_2 CL (B) UV-vis absorption spectra of the TMB/ H_2O_2 , $\text{FeCoNi-MOXs}/\text{TMB}$, and $\text{FeCoNi-MOXs}/\text{TMB}/\text{H}_2\text{O}_2$ systems in 0.2 M NaAc/HAc buffer solution (ACB, pH 4.0). (C) CL intensity–time curves of the luminol/ H_2O_2 system in the absence and presence (red line) of FeCoNi-MOXs. [FeCoNi-MOXs]: 20 $\mu\text{g mL}^{-1}$; [luminol]: 2 μM in CBS (pH 11.0); [H_2O_2]: 20 μM . Reprinted with permission from ref. 62, Copyright 2023 American Chemical Society.

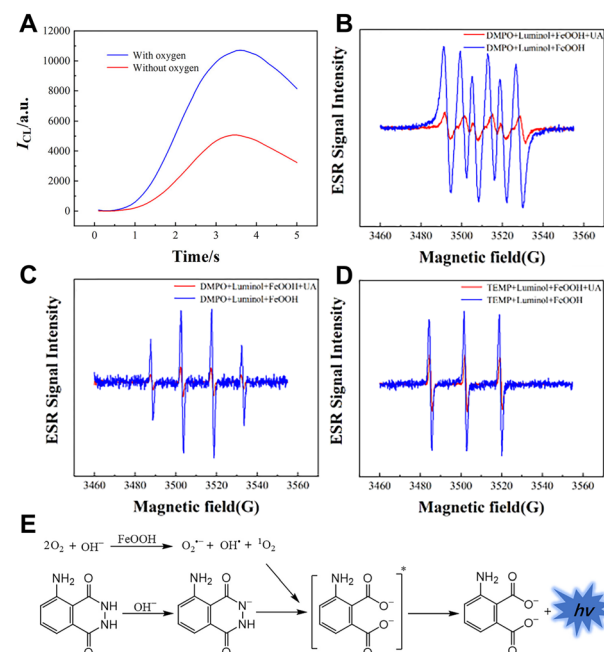


Fig. 12 (A) CL kinetic curves of the luminol/FeOOH system in the absence and presence of oxygen. ESR spectra of adducts. (B) DMPO- $\text{O}_2^{\bullet-}$ (C) DMPO- OH^{\bullet} and (D) TEMP- $^1\text{O}_2$ in the luminol/FeOOH CL system. (E) Mechanism of the luminol/FeOOH CL system. [Luminol]: 100 μM ; [FeOOH]: 25 $\mu\text{g mL}^{-1}$; [UA]: 5 μM ; [pH]: 10.0. Reprinted with permission from ref. 63, Copyright 2023 American Chemical Society.



After deoxygenation, the CL intensity was quenched (Fig. 12A). The electron spin resonance (ESR) spectra (Fig. 12B–D) suggested the formation of hydroxyl radicals (OH^\bullet), $\text{O}_2^\bullet^-$ and singlet oxygen (${}^1\text{O}_2$). Uric acid (UA) can react with these free radicals, enabling the CL detection of UA. The CL mechanism of the luminol/FeOOH NR system is presented in Fig. 12E.

4. CL enhancement driven by mini ultrasound devices

Sonochemiluminescence (SCL), an important subfield of CL, refers to the phenomena of light emission upon chemical reactions of sonolysis products generated from the cavitation bubbles with substances in solution.⁶⁴ Generally, SCL requires ultrasound equipment to drive it. Two main types of

ultrasonication equipment have been used for SCL, including an ultrasonic cleaning bath system and ultrasonic horn system (consisting of the function generator, power amplifier and Langevin-type transducer). However, both of them are expensive, highly energy-consuming and poorly portable, limiting their applications in practical analysis and point-of-care tests.

Inspired by the home USB humidifier, the mesh piezoelectric ultrasonic transducer (MPUT) in the humidifier was reported for luminol SCL for the first time by our group.⁶⁵ The MPUT has the advantages of cost-effectiveness, portability and low-voltage to drive and its components include an atomizing disc and a drive circuit. Both sides of the MPUT atomizing disc are uniformly distributed with micropores (Fig. 13D and E), which helps to enhance the luminol SCL. When energized, the circuit will generate a high-frequency alternating electric field, resulting in the vibration of the piezoelectric ceramic sheet (Fig. 13F). Under high-frequency vibration, the bright blue luminol CL was captured using a smart phone (Fig. 14B). This is due to the reaction between ROS produced from solution under vibration and luminol. Further experiments were conducted to investigate the ROS. Luminol CL was quenched with common free radical scavengers thiourea and SOD, indicating that OH^\bullet and $\text{O}_2^\bullet^-$ were predominantly produced (Fig. 14D). In addition, the central area of the atomizing disc with micropores has stronger luminol CL (Fig. 14B). When the micropores were

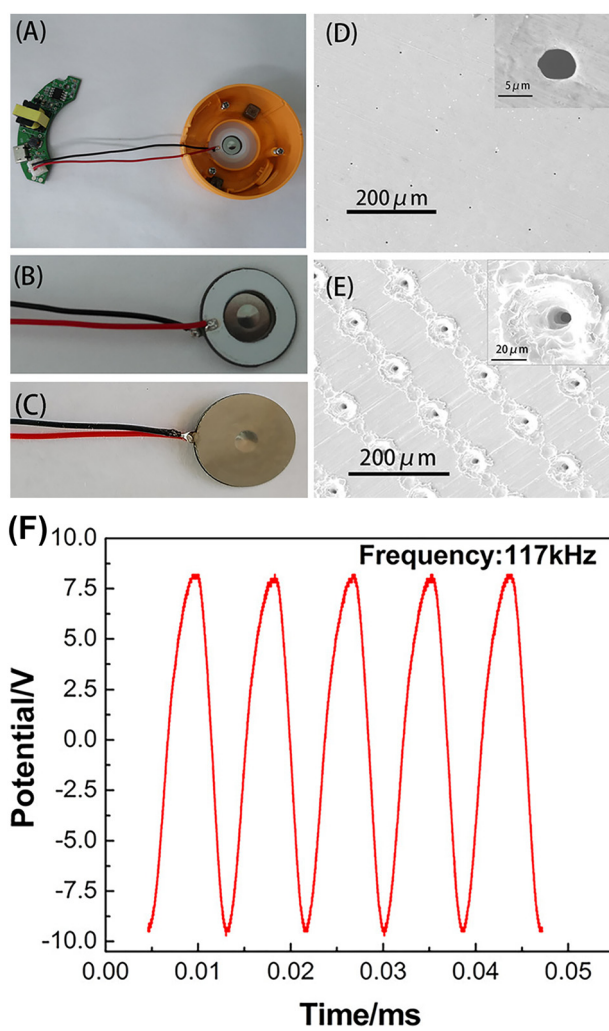


Fig. 13 Schematic representation of an MPUT. (A) The top view of the whole device. Front (B) and back (C) views of the atomizing disc. SEM images of micro-tapered apertures on the front (D) and back (E) sides of the atomizing disc. The insets show the SEM images of a single micro-tapered aperture. (F) Alternating potential–time profile of the MPUT. Reprinted with permission from ref. 65, Copyright 2020 American Chemical Society.

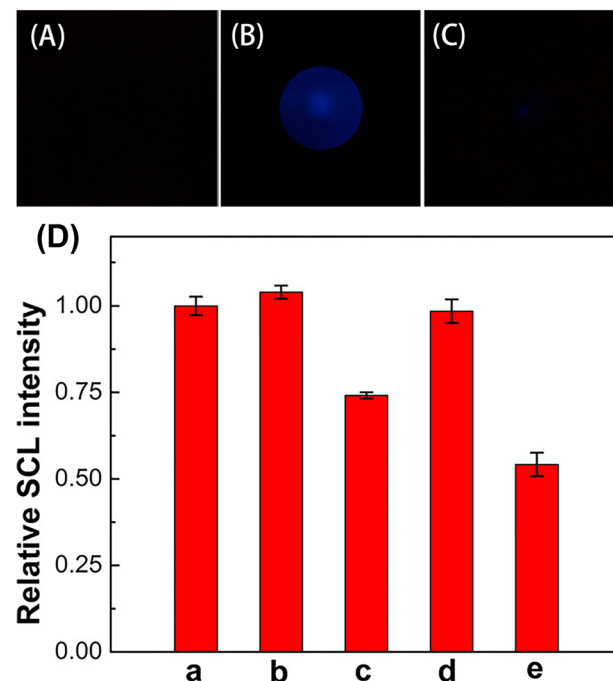


Fig. 14 Images of luminol solution without ultrasonication (A) and under ultrasonication (B). Images of a luminol solution with a micro-tapered aperture sealed MPUT under ultrasonication (C). Effects of radical scavengers on luminol SCL (D). SCL intensity of luminol in the absence (a) and presence of 1.0 mM NaN_3 (b), 1.0 mM thiourea (c), 0.1 $\mu\text{g mL}^{-1}$ SOD (d), and 1.0 $\mu\text{g mL}^{-1}$ SOD (e). [Luminol]: 50 μM ; 0.1 M CBS, pH 12.5; exposure time of the smart phone: 5 s. Reprinted with permission from ref. 65, Copyright 2020 American Chemical Society.



covered, luminol CL was significantly reduced (Fig. 14C). This is because the micropores will enhance the vibration due to the pressure differences caused by high-frequency vibration.

Although the presence of micropores can enhance the CL of luminol, prolonged high-frequency vibration causes the solution to atomize, affecting the stability of the CL signal. Additionally, oxygen can pass through the micropores and affect the CL intensity. Moreover, surfactant-containing solutions and organic solvents can leak through the micropores. Therefore, to improve the universality of the ultrasonic atomizer, a novel piezoelectric ultrasonic transducer (PUT) was

designed by replacing the porous stainless-steel substrate with a non-porous stainless-steel substrate.⁶⁶

The ultrasonic transducer was used to explore the CL of the luminol/H₂O₂ system. In this case, the PUT with micropores showed no significant change in CL intensity with increasing H₂O₂ concentration, while PUT-driven luminol CL signals increased with increasing H₂O₂ concentration (Fig. 15A). This difference is attributed to the improved PUT preventing oxygen from entering the system through the micropores (Fig. 15B and C). H₂O₂ was detected using the improved PUT. H₂O₂ is generated by the reaction between glucose and glucose oxidase. On this basis, the determination of glucose and glucose oxidase activity was achieved using a non-porous PUT.

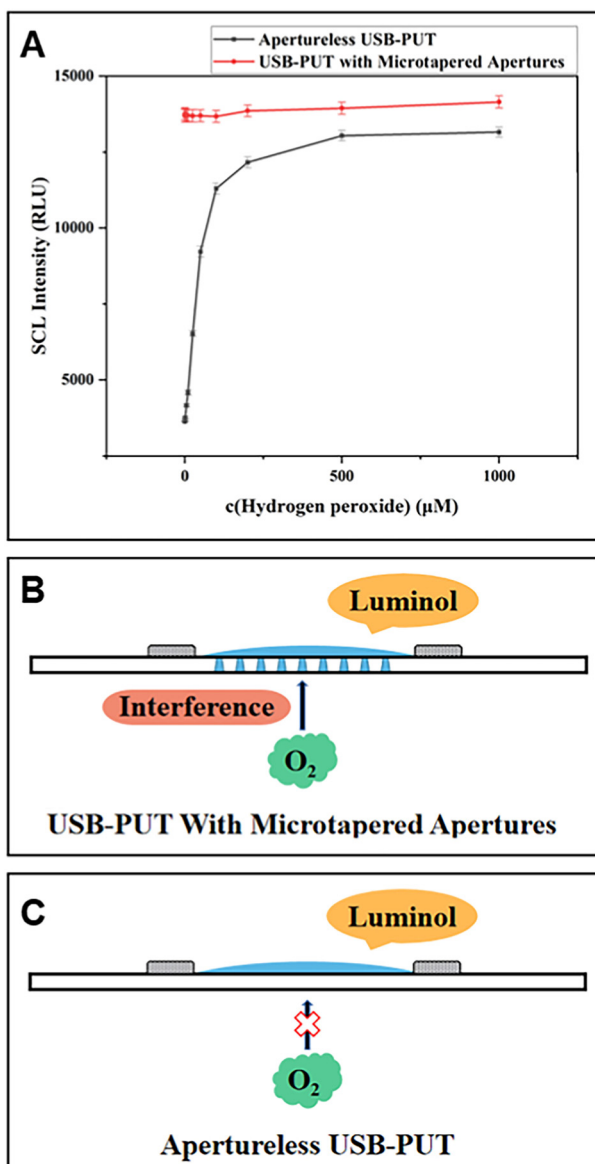


Fig. 15 Comparison between an apertureless USB-PUT and a USB-PUT with microtapered apertures. (A) Effect of H₂O₂ concentration. (B) Principle of the USB-PUT with microtapered apertures. (C) Apertureless USB-PUT. [H₂O₂]: 0.5–1000 μM, [luminol]: 100 μM in pH 12 CBS buffer. Reprinted with permission from ref. 66, Copyright 2021 American Chemical Society.

5. Summary and outlook

In this review, we primarily described our recent efforts to construct basic CL systems and amplify CL signals using nanomaterials and new devices and their analytical applications. We highlighted novel CL systems based on luminol and lucigenin, discussing their mechanisms in detail. To summarize, the principles to construct novel luminol and lucigenin-based CL systems are clear, that is, using substances, nanomaterials or improved devices capable of catalysing the generation of ROS from oxygen, accelerating the production of ROS through H₂O₂ and forming peroxides or oxides *in situ*.

However, despite the CL technique being a powerful analytical tool in many fields, several issues need to be addressed for further development. Firstly, many new CL systems have been developed, which exhibited good CL signals, but most lack selectivity in analytical detection and response to many substances. Therefore, developing CL systems with good selectivity is valuable. Secondly, the development of effective CL systems based on nanomaterials (*e.g.* MXenes, nanoclusters, 2D materials, quantum dots, magnetic nanomaterials, and aggregation-induced emission nanocomposites) and clarification of their working principles are needed. In addition, classical CL systems, such as luminol and lucigenin (light emission under alkaline conditions), remain the most widely used systems. Thus, it is imperative to develop new types of luminophores that work under mild conditions. Furthermore, it is important to develop CL systems emitting near infrared light (NIR) for *in vivo* analysis. Besides, to realize rapid and on-site CL analysis, high-throughput CL systems, as well as miniaturization of CL instruments are indispensable.^{67–69} Finally, combining CL with other technologies, such as artificial intelligence (AI), can further broaden its analytical applications.

Author contributions

Zhiyong Dong: investigation, formal analysis, writing – original draft. Fangxin Du: writing – reviewing and editing. Saima Hanif: writing – reviewing and editing. Yu Tian: writing – reviewing and editing. Guobao Xu: supervision, funding acquisition, project administration, writing – reviewing and editing.



Data availability

No primary research results, software or codes have been included and no new data have been generated or analysed as part of this review.

Conflicts of interest

The authors declare no competing financial interest.

Acknowledgements

This work was financially supported by the National Natural Science Foundation of China (22174136 and 22204160), Natural Science Foundation of Jilin Province (No. YDZJ202201-ZYTS341), Natural Science Foundation of Anhui Provincial Department of Education (No. 2024AH051690), and CAS-TWAS postgraduate fellowship.

References

1. L. Zhao, J. Xu, L. Xiong, S. Wang, C. Yu, J. Lv and J.-M. Lin, *TrAC, Trends Anal. Chem.*, 2023, **166**, 117213.
2. B. R. Radziszewski, *Ber. Dtsch. Chem. Ges.*, 1877, **10**, 70–75.
3. H. O. Albrecht, *Z. Phys. Chem., Stoechiom. Verwandtschaftsl.*, 1928, **136**, 321–330.
4. K. Gleu and W. Petsch, *Angew. Chem.*, 1935, **48**, 0057–0059.
5. F. H. Burstell, *J. Chem. Soc.*, 1936, 173–175.
6. Z. Yi, S. Xiao, X. Kang, F. Long and A. Zhu, *ACS Appl. Mater. Interfaces*, 2024, **16**, 16494–16504.
7. Y. Zhang, M. Li, S. Li and A. Fan, *Talanta*, 2023, **264**, 124748.
8. S. Quan, K. X. Ji, F. S. Liu, T. H. Barkae, M. I. Halawa, S. Hanif, B. H. Lou, J. P. Li and G. B. Xu, *J. Food Drug Anal.*, 2022, **30**, 293–302.
9. W. Yu, X. Zheng, M. Tan, J. Wang, B. Wu, J. Ma, Y. Pan, B. Chen and C. Chu, *Environ. Sci. Technol.*, 2024, **58**, 2808–2816.
10. H. Gong, Y. Zhou, P. Ma, X. Xiao and H. Liu, *ACS Sens.*, 2024, **9**, 2465–2475.
11. I. M. Mostafa, M. Gilani, Y. Q. Chen, B. H. Lou, J. P. Li and G. B. Xu, *J. Food Drug Anal.*, 2021, **29**, 510–520.
12. H. Chen, Y. Feng, F. Liu, C. Tan, N. Xu, Y. Jiang and Y. Tan, *Biosens. Bioelectron.*, 2024, **247**, 115929.
13. F. Qu, J. Shu, S. Wang, M. A. Haghaghbin and H. Cui, *Anal. Chem.*, 2022, **94**, 17073–17080.
14. J. Huang, M. Xu, P. Cheng, J. Yu, J. Wu and K. Pu, *Angew. Chem., Int. Ed.*, 2024, **63**, e202319780.
15. H. Liu, F. Liu, K. Ji, Y. T. Zholudov, I. M. Mostafa, B. Lou, W. Zhang and G. Xu, *Anal. Chem.*, 2023, **95**, 13614–13619.
16. Y. Lan, F. Yuan, T. H. Fereja, C. Wang, B. Lou, J. Li and G. Xu, *Anal. Chem.*, 2019, **91**, 2135–2139.
17. F. Chen, X. Xia, D. Ye, T. Li, X. Huang, C. Cai, C. Zhu, C. Lin, T. Deng and F. Liu, *Anal. Chem.*, 2023, **95**, 5773–5779.
18. W. Zhang, L. Hao, J. Huang, L. Xia, M. Cui, X. Zhang, Y. Gu and P. Wang, *Talanta*, 2019, **201**, 455–459.
19. H. Wu, Y. Fang, L. Tian, X. Liu, X. Zhou, X. Chen, H. Gao, H. Qin and Y. Liu, *ACS Sens.*, 2023, **8**, 3205–3214.
20. S. Tian, C. Peng, H. Xing, Y. Xue, J. Li and E. Wang, *Anal. Chem.*, 2024, **96**, 514–521.
21. Y. Jiang, X. Yang, S. Li, Y. Qiao, Y. Zhou and Y. Li, *Chem. Eng. J.*, 2024, **481**, 148753.
22. M. Yang, J. Huang, J. Fan, J. Du, K. Pu and X. Peng, *Chem. Soc. Rev.*, 2020, **49**, 6800–6815.
23. D. Easwaramoorthy, Y.-C. Yu and H.-J. Huang, *Anal. Chim. Acta*, 2001, **439**, 95–100.
24. J. I. Creamer, T. I. Quickenden, M. V. Apanah, K. A. Kerr and P. Robertson, *Luminescence*, 2003, **18**, 193–198.
25. N. Ma, Z. Zhang, F. Liao, T. Jiang and Y. Tu, *Pharmacol. Ther.*, 2020, **216**, 107658.
26. C. Wang, M. I. Halawa, B. Lou, W. Gao, J. Li and G. Xu, *Analyst*, 2021, **146**, 1981–1985.
27. W. Gao, C. Wang, K. Muzyka, S. A. Kitte, J. Li, W. Zhang and G. Xu, *Anal. Chem.*, 2017, **89**, 6160–6165.
28. W. Gao, W. Qi, J. Lai, L. Qi, S. Majeed and G. Xu, *Chem. Commun.*, 2015, **51**, 1620–1623.
29. F. Liu, K. Ji, S. Quan, Z. Zhou, Z. Dong, A. Hussain, W. Zhang and G. Xu, *Chem. Commun.*, 2022, **58**, 10214–10217.
30. M. D. Green, D. L. Mount, G. D. Todd and A. C. Capomacchia, *J. Chromatogr. A*, 1995, **695**, 237–242.
31. D. J. Bowles, A. S. Olson, N. H. Hodges, D. L. Heglund, R. L. Vargas and S. A. Williams, *Appl. Spectrosc.*, 2012, **66**, 175–179.
32. T. H. Fereja, S. A. Kitte, W. Gao, F. Yuan, D. Snizhko, L. Qi, A. Nsabimana, Z. Liu and G. Xu, *Talanta*, 2019, **204**, 379–385.
33. Z. Kis, S. V. Makarov and R. Silaghi-Dumitrescu, *J. Sulfur Chem.*, 2010, **31**, 27–39.
34. A. Safavi and M. A. Karimi, *Talanta*, 2002, **57**, 491–500.
35. M. Saqib, S. Li, W. Gao, S. Majeed, L. Qi, Z. Liu and G. Xu, *Anal. Bioanal. Chem.*, 2016, **408**, 8851–8857.
36. S. M. Derayea and E. Samir, *Microchem. J.*, 2020, **156**, 104835.
37. C. Wang, Y. Chen, D. Snizhko, F. Du, X. Ma, B. Lou, J. Li and G. Xu, *Talanta*, 2020, **218**, 121177.
38. X. Zhou, J. Jiao, W. Jiao and R. Wang, *Sep. Purif. Technol.*, 2023, **310**, 123180.
39. G. Yang, X. Xie, M. Cheng, X. Gao, X. Lin, K. Li, Y. Cheng and Y. Liu, *Chin. Chem. Lett.*, 2022, **33**, 1483–1487.
40. D. Bajuk-Bogdanovic, I. Holclajtner-Antunovic, M. Todorovic, U. B. Mioc and J. Zakrzewska, *J. Serb. Chem. Soc.*, 2008, **73**, 197–209.
41. M. T. Pope and G. M. Varga, Jr., *Inorg. Chem.*, 1966, **5**, 1249–1254.
42. I. M. Mostafa, M. I. Halawa, Y. Chen, A. Abdussalam, Y. Guan and G. Xu, *Analyst*, 2020, **145**, 2709–2715.
43. W. Gao, L. Qi, Z. Liu, S. Majeed, S. A. Kitte and G. Xu, *Sens. Actuators, B*, 2017, **238**, 468–472.
44. M. Saqib, B. Lou, M. I. Halawa, S. A. Kitte, Z. Liu and G. Xu, *Anal. Chem.*, 2017, **89**, 1863–1869.
45. A. Abdussalam, Y. Chen, F. Yuan, X. Ma, B. Lou and G. Xu, *Anal. Chem.*, 2022, **94**, 11023–11029.
46. H. Zhu, X. Huang, Y. Deng, H. Chen, M. Fan and Z. Gong, *TrAC, Trends Anal. Chem.*, 2023, **158**, 116879.
47. Y. Yan, X.-y. Wang, X. Hai, W. Song, C. Ding, J. Cao and S. Bi, *TrAC, Trends Anal. Chem.*, 2020, **123**, 115755.
48. Y. Peng, L. Yu, M. Sheng, Q. Wang, Z. Jin, J. Huang and X. Yang, *Anal. Chem.*, 2023, **95**, 18436–18442.
49. C. Huang, W. Zhou, W. Guan and N. Ye, *Anal. Chim. Acta*, 2024, **1295**, 342324.
50. T. C. Wareing, P. Gentile and A. N. Phan, *ACS Nano*, 2021, **15**, 15471–15501.
51. L. Zhao, F. Di, D. Wang, L.-H. Guo, Y. Yang, B. Wan and H. Zhang, *Nanoscale*, 2013, **5**, 2655–2658.
52. C. Wang, Y. Lan, F. Yuan, T. H. Fereja, B. Lou, S. Han, J. Li and G. Xu, *Microchim. Acta*, 2019, **187**, 50.
53. I. Zare, D. Choi, J. Zhang, M. T. Yaraki, A. Ghaee, S. Z. Nasab, R. Taheri-Ledari, A. Maleki, A. Rahi, K. Fan and J. Lee, *Nano Today*, 2024, **56**, 102276.
54. Y. Ai, Z.-N. Hu, X. Liang, H.-b Sun, H. Xin and Q. Liang, *Adv. Funct. Mater.*, 2022, **32**, 2110432.
55. H. Chai, K. Yu, Y. Zhao, Z. Zhang, S. Wang, C. Huang, X. Zhang and G. Zhang, *Anal. Chem.*, 2023, **95**, 10785–10794.
56. D. Lu, M. Ge, F. Qian, J. Lv and J. Du, *Microchim. Acta*, 2024, **191**, 200.
57. X. J. Yang, R. S. Li, C. M. Li, Y. F. Li and C. Z. Huang, *Talanta*, 2020, **215**, 120928.
58. Y. Gao, Y. Huang, J. Chen, Y. Liu, Y. Xu and X. Ning, *Anal. Chem.*, 2021, **93**, 10593–10600.
59. P. Hao, Y. Liu, L. Wang, X. Zhu and Q. Liu, *ACS Appl. Nano Mater.*, 2023, **6**, 1937–1947.
60. Z. Wang, P. Ju, Y. Zhang, F. Jiang, H. Ding and C. Sun, *Microchim. Acta*, 2020, **187**, 424.
61. Z. Dong, S. Xia, A. a M. A. Alboull, I. M. Mostafa, A. Abdussalam, W. Zhang, S. Han and G. Xu, *ACS Appl. Nano Mater.*, 2024, **7**, 2983–2991.
62. F. Liu, S. Xia, A. a M. A. Alboull, Z. Dong, H. Liu, C. Meng, F. Wu and G. Xu, *Anal. Chem.*, 2023, **95**, 9380–9387.
63. K. Ji, S. Xia, X. Sang, A. M. Zeid, A. Hussain, J. Li and G. Xu, *Anal. Chem.*, 2023, **95**, 3267–3273.
64. E. N. Harvey, *J. Am. Chem. Soc.*, 1939, **61**, 2392–2398.
65. F. Du, X. Ma, F. Yuan, C. Wang, D. Snizhko, Y. Guan and G. Xu, *Anal. Chem.*, 2020, **92**, 4755–4759.



66 C. Meng, F. Du, A. Abdussalam, A. Wang, D. Snizhko, W. Zhang and G. Xu, *Anal. Chem.*, 2021, **93**, 14934–14939.

67 C. Meng, S. Knežević, F. Du, Y. Guan, F. Kanoufi, N. Sojic and G. Xu, *eScience*, 2022, **5**, 591–605.

68 X. Ma, W. Gao, F. Du, F. Yuan, J. Yu, Y. Guan, N. Sojic and G. Xu, *Acc. Chem. Res.*, 2021, **54**, 2936–2945.

69 H. Liu, A. Hussain, Y. Zholudov, D. Snizhko, N. Sojic and G. Xu, *Angew. Chem., Int. Ed.*, 2024, **63**, e202411764.

